

Magnetic domains in Co thin films obliquely sputtered on a polymer substrate

A. Lisfi* and J. C. Lodder

Information Storage Technology Group, MESA⁺ Research Institute, University of Twente, P.O. Box 217,
7500 AE Enschede, The Netherlands

(Received 19 July 2000; revised manuscript received 30 January 2001; published 16 April 2001)

Magnetic domains in obliquely sputtered Co films on a polymer substrate have been investigated with magnetic force microscopy. The growth angle has been found to strongly affect the domain structure as well as the magnetic properties, due to changes in the microstructure. At large angles finite-size elongated domains oriented in the longitudinal direction (projection of the growth direction on the film plane) were energetically favorable. However, at intermediate angles a transition to stripe domains occurs due to an increase in exchange coupling. These domains exhibit a width of 400 nm and lie along the longitudinal direction. In the remanent state (after saturation), circular as well as elliptical magnetic bubbles coexist, but coalesce in the dc demagnetized state to form stripe domains.

DOI: 10.1103/PhysRevB.63.174441

PACS number(s): 75.70.Kw, 75.60.-d, 81.15.Ef

Oblique deposition (evaporation^{1,2} as well as sputtering) is one of the most promising methods for growing metallic magnetic thin films for high-density tape recording applications. The morphology of films grown with this technology exhibits a columnar structure that is mainly due to the shadow effect. The columns are tilted at an angle to the plane normal, depending on the incident angle of the incoming atoms.^{3,4} The columnar structure can have an important role in the control of the magnetic properties of the film because of the additional anisotropy due to the shape of the columns. This magnetic anisotropy is efficient only if the columns exhibit a low exchange coupling, resulting in a large tilt in the easy axis from the film plane. However, if the columns are strongly coupled, the shape anisotropy of the film ($-\mu_0 M_s^2/2$) prevails and tries to confine the easy axis as close as possible to the film plane. Exchange coupling may also induce other effects, such as a reduction in coercivity and an increase in media noise during magnetic recording and read-back. A reduction in exchange coupling may be achieved by the oxidation of the metallic film by supplying oxygen during growth. It has been confirmed that oxide surrounds the metallic columns thus reducing exchange coupling.^{5,6} Furthermore, the contact between the antiferromagnetic phase (oxide) and the columns generates a unidirectional anisotropy, resulting in a shift of the hysteresis loop.⁷ This shift has been clearly observed at low temperatures for Co-Ni evaporated tapes.⁸

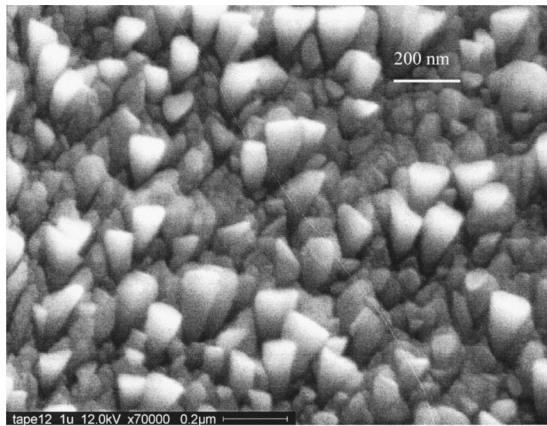
Due to the potential application of such kind of media in longitudinal magnetic recording, dependence on incidence angle of magnetic properties such as in-plane anisotropy, coercivity, remanence, and tilt of easy axis have been the subject of intensive research.⁹⁻¹⁴ Most of these studies reveal and agree on the following points: (a) Below 50°, the coercivity (H_c) is very low and exhibits a smooth change with the angle. At large angle, H_c shows a very fast increase. (b) The squareness increases with the incidence angle. (c) By varying the incidence angle, a reorientation of anisotropy occurs. At large angle, the easy axis of the magnetization is confined to the incidence plane, whereas at intermediate angle (less than 50°) the anisotropy switches to be parallel to the transverse direction. As the most important variation of

anisotropy occurs at incidence angle larger than 40°, it seems to be interesting to explore the structure of magnetic domains in this angular region.

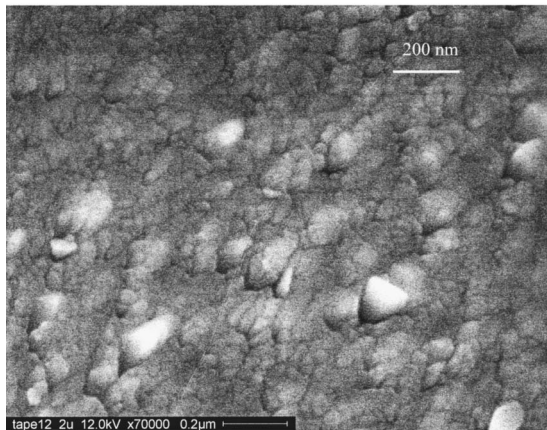
In this paper, we report on the observation of stripe as well as elongated domains oriented along the longitudinal direction in Co thin films. Many studies have been made of the magnetic properties of Co, both as very thin films¹⁵ as well as multilayers.¹⁶ The development of new imaging techniques such as secondary electron microscopy with polarization analysis (SEMPA) and magnetic force microscopy (MFM) has allowed the investigation of the domain structure in very thin films of Co (few monolayers). With SEMPA, it has clearly been established that the transition of the magnetization from out-of-plane to in-plane occurs at a 3.5 ML thickness of Co.¹⁷ Recently, magnetic domains in a set of Co films grown by molecular beam epitaxy on sapphire at 300 °C and possessing a large range of thicknesses (10–500 nm), have been studied with MFM.¹⁸ These films exhibited a hcp structure, however, the anisotropy orientation switched to the perpendicular direction of the film plane above a critical thickness, as predicted by Kittel.¹⁹

In this study, Co films have been grown by oblique sputtering on a polymer substrate (polyethylene terephthalate) as small samples (10×5 cm²) of magnetic tape. The samples were prepared in a mini roll-coater consisting of a solid drum. A static configuration was used with continuous varying incidence (CVI). All the films were deposited at room temperature and at the same residual pressure (4 × 10⁻³ mb). In order to analyze the structural and the magnetic properties of the films, five 1 × 1 cm² samples were cut from different areas of the Co tape, at positions corresponding to different growth angles. More details about the film preparation will be published elsewhere.²⁰

The film microstructure was studied with a high-resolution scanning electron microscope (SEM) as well as an atomic force microscope (AFM). Figure 1(a) shows an SEM image of a Co film, 125 nm thick, sputtered at 70° to the surface normal (sample A). The film microstructure consists of large columns with triangular shape, oriented in the plane of incidence. These columns are well separated, but in most cases are surrounded by clusters of small columns. The anisotropic behavior of this microstructure is mainly due to the



(a)

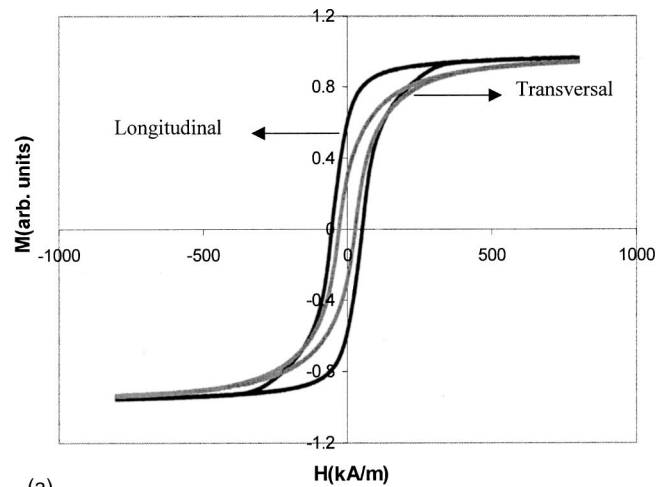


(b)

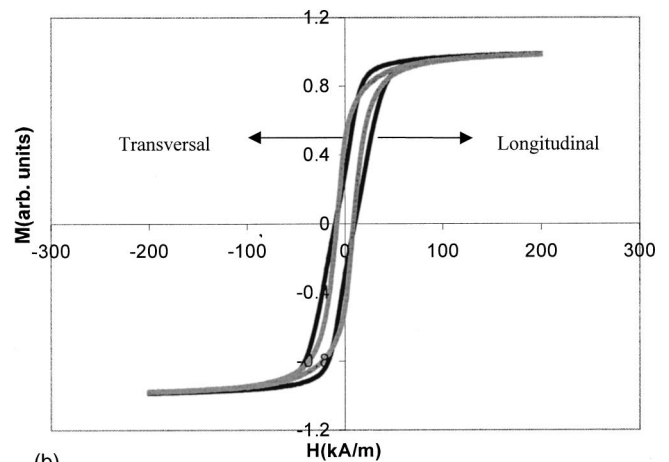
FIG. 1. (a) SEM image of a Co film grown on PET at 70° from the normal to the film plane (sample A). The columns exhibit a triangular shape and lie in the incidence plane. (b) SEM image of a Co film grown at 50° as incidence angle (sample B). The shadow effect is less important than for sample A, with a more continuous morphology being observed.

oblique deposition angle, which favors growth in a certain direction. Figure 1(b) is an SEM image of a 300-nm-thick film (sample B), taken from the same deposition run as for sample A, but grown at a lower angle (50°). Although the two samples originate from the same Co tape, they possess different film thicknesses due to the static configuration during growth. Sample B is thicker due to being closer to the deposition source. The morphology of sample B seems to be more continuous with a smooth surface and grains very close to each other. The difference in the microstructures shown in the two images [Figs. 1(a) and 1(b)] is mainly caused by the shadow effect, which increases with the angle of incidence.

The magnetic properties of the films were measured with a VSM and a torque magnetometer. Figure 2(a) shows the hysteresis loops measured in the film plane in both longitudinal and transverse directions of sample A. The longitudinal loop exhibits a high coercivity ($H_c = 55$ kA/m) and a large remanence ($M_r/M_s = 0.8$), whereas these two parameters are quite low in the transverse direction ($H_c = 30$ kA/m, $M_r/M_s = 0.4$). In order to investigate the magnetic anisotropy of the films, two kinds of measurements have been



(a)



(b)

FIG. 2. (a) Longitudinal and transverse hysteresis loops of Co deposited at 70° (sample A). The large difference in the coercivity is due to the shape anisotropy of the columns, which exhibit a low exchange coupling. (b) Longitudinal and transverse hysteresis loops of Co deposited at 50° (sample B). Both loops possess similar coercivities.

performed with the torque magnetometer. The first consists of rotating the field from the normal to the film plane, whereas in the second the field is rotated in the film plane, from the longitudinal to the transverse direction. The results of the first experiment reveal that the easy axis is tilted about 10° from the film plane. However, in the second measurement, a uniaxial anisotropy ($K_u = 5.6 \times 10^4$ J/m³) with easy and hard axes is observed along the longitudinal and the transverse directions, respectively. Figure 2(b) shows two hysteresis loops for sample B. There is no significant difference in the coercivities measured in the two directions ($H_c = 12$ and 10 kA/m for the longitudinal and the transverse directions, respectively). This result is in good agreement with the torque measurements that revealed a very low anisotropy in the film plane ($K_u = 2.7 \times 10^3$ J/m³) for this sample. However, a small tilt in the easy axis was found (4°). A comparison of the results for both films reveals that the magnetic properties are strongly affected by the microstructure. The greater coercivity as well as the large tilt of the

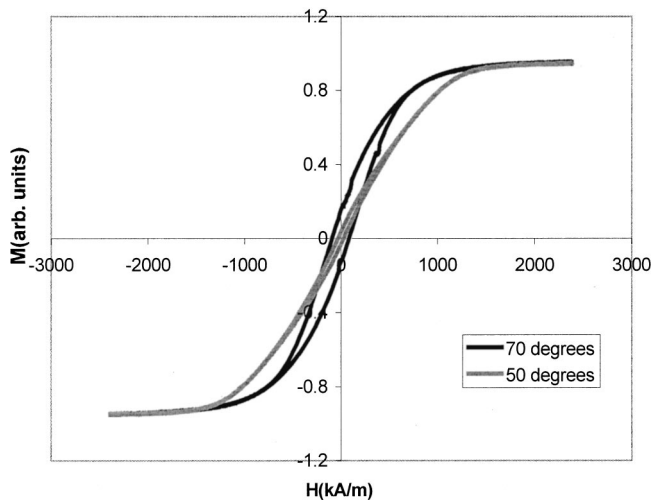
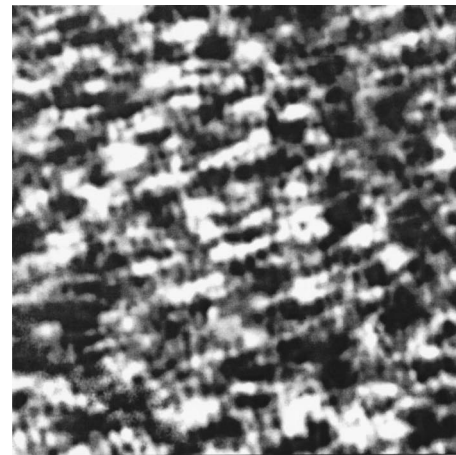


FIG. 3. Perpendicular loops of both films grown at 50° and 70° incidence angle. At large angle (70°), the hysteresis is much pronounced, whereas the shearing of the loop and saturation field are largely reduced.

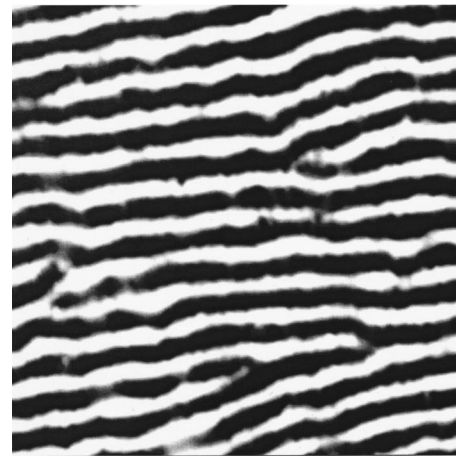
easy axis for sample *A* are mainly induced by the shape anisotropy of the columns. The columns appear to be more isolated, as confirmed by the SEM image shown in Fig. 1(a). The shadow effect is less pronounced for sample *B*, grown at 50°, resulting in the columns being more closely packed. The main reason, which can explain the low tilt in the easy axis (4°), is the strong exchange coupling between the columns. Such coupling reduces the influence of any shape anisotropy resulting from the collective behavior of clusters of columns on the magnetization process. The magnetic anisotropy of the film ($-\mu_0 M_s^2/2$) is favored, taking the film plane as the preferential direction.

The hysteresis loops measured with the field perpendicular to the film plane reveal two clear results (Fig. 3): (1) The shearing in the loop as well as the field necessary to saturate the magnetization are much lower for sample *A* than for sample *B*. (2) The hysteresis is more pronounced for sample *A*. The difference in the shearing of perpendicular loops and saturation fields can be explained by the variation in the magnetization due to the column packing density, which is strongly dependent on the incident angle. However, the large hysteresis shown in the perpendicular loop of sample *A* is mainly due to the large tilt of the easy axis (10°), because of the important contribution of individual columns to the magnetization process (low exchange coupling). Other parameters such as the remanent coercivity and the width of the switching-field distribution have been deduced from DCD remanence curves and found to be strongly influenced by the microstructure. In fact, the remanence measurements were found to be dependent on the demagnetizing field, which is also related to the column structure.

The imaging of the magnetic domains was performed with a commercial MFM (Digital Instruments, DI 3100) operated in tapping liftmode. This ensures a clear separation between the topographic and magnetic data. A commercial Si tip coated with a ~30-nm-thick CoCr thin film that was magnetized vertically was used. The tip-to-sample distance



(a)



(b)

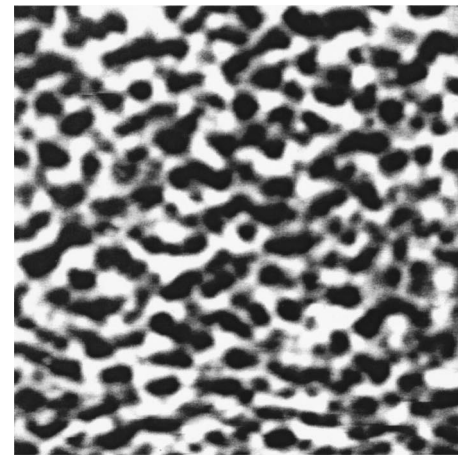
FIG. 4. (a) MFM image ($10 \times 10 \mu\text{m}^2$) of Co grown at 70° (sample *A*), showing two kinds of domains (elongated in the longitudinal direction and circular). (b) $10 \times 10 \mu\text{m}^2$ MFM image of Co, grown at 50° (sample *B*), showing a striped domain structure. The sample was ac demagnetized. The domains are oriented in the longitudinal direction, which corresponds to the easy axis in the film plane as revealed by torque measurements.

was approximately 100 nm during magnetic imaging. The MFM image contrast is proportional to the gradient of the magnetic force between tip and sample. Figure 4(a) is an MFM image of sample *A*. The magnetic domains exhibit an elongated shape, oriented along the longitudinal direction. Additionally, smaller magnetic domains are also clearly observed. The coexistence of these two kinds of domains is due to the nonuniformity of the exchange coupling in the film. The microstructure shown in Fig. 1(a) reveals the existence of big columns isolated from each other and surrounded by clusters of small grains. The exchange coupling in the clusters can give rise to large domains while the small circular domains can be attributed to the large isolated columns. The orientation of the elongated domains can be explained by the existence of a large magnetic anisotropy ($K_u = 5.6 \times 10^4 \text{ J/m}^3$) in the film plane. In Fig. 4(b) an MFM image of sample *B* shows stripe domains oriented along the longitudinal direction. This image is of the sample in an ac demagnetized state. The width of the domains is estimated to be 400

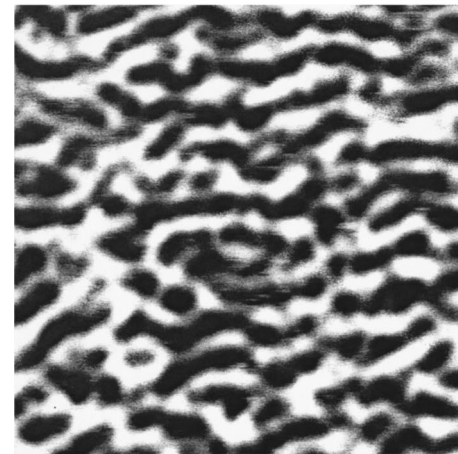
nm. A comparison of Figs. 4(a) and 4(b) reveals that uniform exchange coupling favors stripe domains, whereas slow and nonuniform exchange coupling due to a large shadow effect induces small domains. This can explain the large difference in the coercivity between the two samples.

Stripe domains in obliquely evaporated materials have been classified into two types (1 and 2) or weak and strong.^{21–24} There are two major differences between these two categories: (1) the weak stripe domains (type 1) appear when a field is applied, whereas the stronger (type 2) domains are favored for samples in a demagnetized state^{21,22}; (2) type 2 domains lie in the growth plane, while type 1 domains are aligned almost perpendicular to this plane. The structure of the domains observed in Fig. 4(b) belongs to category 2 (strong stripe domains). It is interesting to note that the tilt of the easy axis from the film plane is very small (4°), which implies that the in-plane component of the magnetization makes the largest contribution to the contrast in the MFM image.

Figure 5(a) is an MFM image of sample *B*; in contrast to Fig. 4(b) the sample was imaged while in a remanent state after saturation in the longitudinal direction. It is clear that the magnetic structure is composed of circular as well as elongated bubbles, which form a stable configuration typical of the remanent state. It has been established by many authors^{25,26} that the observation of a singularity in the magnetization loop of perpendicular medium, when the field is reduced from the saturation, may be taken as evidence of bubble formation. Generally, the bubbles exhibit a circular shape on nucleation; however, it has been shown by Thiele²⁷ that this shape changes to an ellipse during bubble growth. It is clear from Fig. 5(a) that the bubbles grow along the longitudinal direction. This can be explained by the existence of a magnetic anisotropy in the film plane, as revealed by the torque measurements. Figure 5(b) shows the domain structure of sample *B* in a dc demagnetized state. In this case, the sample was first saturated in the longitudinal direction, subsequently a field equal to the remanent coercivity ($H_r = 11.5$ kA/m) was applied in the opposite direction and then removed. The domain structure revealed in Fig. 5(b) appears to be a development of that shown in Fig. 5(a), in which the bubbles have grown as the field is applied, and coalesce to form stripe domains. Although the dc demagnetized state [Fig. 5(a)] reveals a structure with stripe domains, a net difference can be observed between the images shown in Figs. 4(b) and 5(b). It is important to mention that for perpendicular media, the structure of the stripe domains depends on the direction of the demagnetizing field. Domains are oriented either parallel to the field or randomly for in-plane or perpendicular demagnetizing fields. However, for the samples



(a)



(b)

FIG. 5. (a) $10 \times 10 \mu\text{m}^2$ MFM image of sample *B*, measured in the remanent state after saturation in the longitudinal direction. The two kinds of bubbles (circular and elliptic) coexist and form a stable state. (b) $10 \times 10 \mu\text{m}^2$ MFM image of sample *B* following dc demagnetization in the longitudinal direction.

discussed here, the stripe domains lie in the longitudinal direction in all the cases due to the in-plane anisotropy.

In summary, a transition from elongated to stripe magnetic domains, depending upon growth angle, has been observed for Co thin films obliquely sputtered on a polymer substrate. Circular as well as elliptic magnetic bubbles coexist in the remanent state, coalescing in the dc demagnetized state to form stripe domains parallel to the longitudinal direction.

The authors would like to thank Dr. G. N. Phillips for his helpful comments.

*Corresponding author. FAX: +31-53-489-3343. Email address: a.lisfi@el.utwente.nl

¹T. G. Knorr and R. W. Hoffman, Phys. Rev. **113**, 1039 (1959).

²D. O. Smith, M. S. Cohen, and J. P. Weiss, J. Appl. Phys. **31**, 1755 (1960).

³S. L. Zeder, J.-F. Silvain, M. E. Re, M. H. Kryder, and C. L. Bauer, J. Appl. Phys. **61**, 3804 (1987).

⁴Seth Lichter and Jyhmin Chen, Phys. Rev. Lett. **56**, 1396 (1986).

⁵J. S. Gau, R. G. Spahn, and D. Majumdar, IEEE Trans. Magn. **22**, 582 (1986).

⁶D. Majumdar, J. S. Gau, and R. G. Spahn, Thin Solid Films **145**, 241 (1986).

⁷W. Meiklejohn *et al.*, Phys. Rev. **105**, 904 (1957).

⁸Peter Ten Berge, Leon Abelmann, Cock Lodder, Ab Schrader,

- and Steven Luitjens, *J. Magn. Soc. Jpn.* **18** (Suppl S1), 295 (1994).
- ⁹Huei-Mi Ho, George J.-S. Gau, and Gareth Thomas, *J. Appl. Phys.* **65**, 3161 (1989).
- ¹⁰D. E. Speliotis, G. Bate, J. K. Alstad, and J. R. Morrison, *J. Appl. Phys.* **36**, 972 (1965).
- ¹¹Eiji Kita, Kimeteru Tagawa, Masafumi Kamikubota, and Akira Tasaki, *IEEE Trans. Magn.* **17**, 3193 (1981).
- ¹²Y. Hoshi and M. Naoe, *IEEE Trans. Magn.* **24**, 3015 (1988).
- ¹³Takashi Hashimoto, Kazuhiro Hara, Takashi Hashimoto, Kunito Okamoto, and Hiroshi Fujiwara, *J. Phys. Soc. Jpn.* **34**, 1415 (1973).
- ¹⁴S. Keitoku, S. Negishi, I. Tsuchitori, and M. Goto, *IEEE Trans. Magn.* **5**, 1114 (1990).
- ¹⁵C. M. Schneider, P. Bressler, P. Schuster, J. Kirschner, J. de Miguel, and R. Miranda, *Phys. Rev. Lett.* **64**, 1059 (1990).
- ¹⁶S. S. P. Parkin, Z. G. Li, and J. Smith, *Appl. Phys. Lett.* **58**, 2710 (1991).
- ¹⁷R. Allenspach, M. Stampanoni, and A. Bischof, *Phys. Rev. Lett.* **65**, 3344 (1990).
- ¹⁸M. Hehn, S. Padovani, K. Ounadjela, and J. P. Bucher, *Phys. Rev. B* **54**, 3428 (1996).
- ¹⁹C. Kittel, *Phys. Rev.* **70**, 965 (1946).
- ²⁰A. Lisfi and J. C. Lodder (unpublished).
- ²¹Eiji Tatsumoto and Kazuhiro Hara, *Jpn. J. Appl. Phys.* **7**, 176 (1968).
- ²²K. Hara, *J. Sci. Hiroshima Univ., Ser. A-2* **34**, 139 (1970).
- ²³R. J. Spain, *Appl. Phys. Lett.* **3**, 208 (1963).
- ²⁴N. Saito, H. Fujiwara, and Y. Sugita, *J. Phys. Soc. Jpn.* **19**, 421 (1964).
- ²⁵C. Kooy and U. Enz, *Philips Res. Rep.* **15**, 7 (1960).
- ²⁶J. A. Cape and G. W. Lehman, *J. Appl. Phys.* **42**, 5732 (1971).
- ²⁷A. A. Thiele, *Bell Syst. Tech. J.* **50**, 725 (1971).